

Generalised Medical Phrase Grounding

Wenjun Zhang, Shekhar S. Chandra, and Aaron Nicolson

Abstract—Medical phrase grounding (MPG) maps textual descriptions of radiological findings to corresponding image regions. These grounded reports are easier to interpret, especially for non-experts. Existing MPG systems mostly follow the referring expression comprehension (REC) paradigm and return exactly one bounding box per phrase. Real reports often violate this assumption. They contain multi-region findings, non-diagnostic text, and non-groundable phrases, such as negations or descriptions of normal anatomy. Motivated by this, we reformulate the task as generalised medical phrase grounding (GMPG), where each sentence is mapped to zero, one, or multiple scored regions. To realise this formulation, we introduce the first GMPG model: MedGrounder. We adopted a two-stage training regime: pre-training on report sentence–anatomy box alignment datasets and fine-tuning on report sentence–human annotated box datasets. Experiments on PadChest-GR and MS-CXR show that MedGrounder achieves strong zero-shot transfer and outperforms REC-style and grounded report generation baselines on multi-region and non-groundable phrases, while using far fewer human box annotations. Finally, we show that MedGrounder can be composed with existing report generators to produce grounded reports without retraining the generator.

I. INTRODUCTION

Medical phrase grounding (MPG) maps textual descriptions of radiological findings to spatial regions in medical images. Presenting findings with their associated bounding boxes allows the text to be easier to interpret, especially by non-experts [1]–[3]. Despite their promise, contemporary MPG systems exhibit several notable limitations. Most methods follow the referring expression comprehension (REC) framework, originally designed for general-domain phrase grounding. As shown in Figure 1 (top left), the model takes an image and phrase as input and predicts a bounding box by regressing its coordinates, creating a one-to-one mapping between each phrase and region [1], [2]. However, this assumption is fundamentally misaligned with the visual presentation of clinical findings. Radiology reports contain findings corresponding to multiple regions (e.g., “bilateral lower lobe opacities”), phrases that should not be grounded, including negated findings (e.g., “No pneumothorax”), descriptions of normal anatomy, and non-diagnostic text like “PA views provided”. Existing REC-based approaches, such as MedRPG [2] and AGPT [1], cannot handle these cases.

W. Zhang (e-mail: wenjun.zhang@uq.net.au) and S. S. Chandra are with The University of Queensland, Brisbane, Australia; W. Zhang and A. Nicolson are with the Australian e-Health Research Centre, CSIRO Health and Biosecurity, Australia.

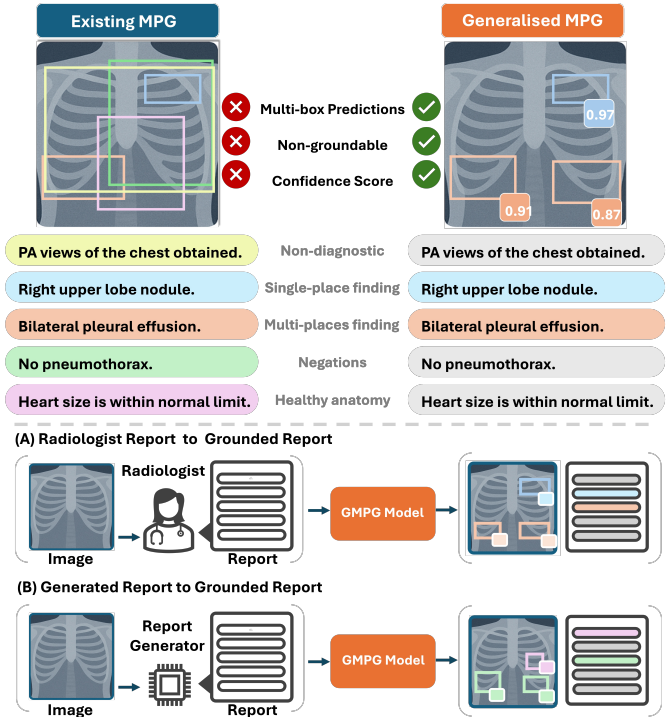


Fig. 1. Top: MPG predicts a single bounding box per sentence, while GMPG additionally supports (i) multiple boxes per sentence, (ii) suppression of boxes for non-groundable phrases (e.g., negations), and (iii) confidence scoring for all predictions. **Bottom:** Applications of GMPG: (A) grounding a radiologist-written report for patient comprehension, and (B) grounding an AI-generated report for radiologist verification.

Recent formulations of phrase grounding are more flexible—generalised referring expression comprehension (GREC) treats grounding as a set prediction problem rather than single-box regression [4], [5]. Inspired by GREC, we address the weaknesses of MPG by introducing generalised MPG (GMPG), a re-definition of MPG that explicitly supports zero-or-more region grounding with confidence scores. To realise this formulation, we propose MedGrounder, a detection Transformer model adapting MDETR [6] to the medical domain. We adopt a two-stage training strategy. First, we pretrain MedGrounder on a processed version of the Chest ImageGenome dataset [7], which has report sentences linked to anatomical bounding boxes. A large language model was used to process the dataset in order to link the sentences to the anatomical regions and to remove redundant regions. Second, we fine-tune and evaluate the model on expert-annotated datasets, including MS-CXR [8] and PadChest-GR [9].

MedGrounder also enables grounded report generation (GRG) when paired with existing report generators, as shown

TABLE I

COMPARISON OF PRIOR WORK BASED ON GMPG REQUIREMENTS. THE TABLE POSITIONS EXISTING MEDICAL PHRASE GROUNDING AND RELATED MODELS AGAINST THE THREE CORE REQUIREMENTS OF GMPG: **MULTI-REGION** (SUPPORT FOR ZERO, ONE, OR MULTIPLE REGIONS PER PHRASE), **GROUNDABILITY** (ABILITY TO ABSTAIN FROM GROUNDING), AND **CONFIDENCE** (PROVISION OF CONFIDENCE SCORES FOR PREDICTIONS).

Method	Year-venue	Box supervision	Learning paradigm	Multi-region	Groundability	Confidence
GLoRIA	2021-ICCV	No	Contrastive	✓	×	×
BioViL	2022-ECCV	No	Contrastive	✓	×	×
LDM	2024-JBHI	No	Diffusion	✓	×	×
Generate to Ground	2025 MIDL	No	Diffusion	✓	×	×
MedRPG	2023-MICCAI	Yes	MPG / REC	×	×	×
VG-CT	2023-MICCAI	Yes	Multi-task	×	×	×
ChEX	2024-ECCV	Yes	Multi-task	✓	×	✓
MedRG	2024-CORR	Yes	Multi-task	×	×	✓
MAIRA-2	2024	Yes	GRG	✓	✓	×
AGPT	2025-ISBI	Yes	MPG / REC	×	×	×
MedGrounder (ours)	2025	Yes	GMPG / GREC	✓	✓	✓

in Figure 1 (bottom). Although automatic report generation has been widely studied, clinical deployment remains limited. One reason is that radiologists must still verify model outputs due to insufficient accuracy and safety concerns [10]. GRG helps by highlighting visual evidence for each reported finding in the image, which makes verification easier for radiologists [11]. Furthermore, training grounded radiology report generators typically requires large scale image-report-box data that is expensive to obtain. Alternatively, MedGrounder can be applied to a generated report to produce a grounded version. This decoupled approach bypasses the data-annotation bottleneck while remaining compatible with state-of-the-art generators.

Contributions:

- We formulate **Generalised Medical Phrase Grounding (GMPG)**, a set prediction task that extends MPG to allow zero, one, or multiple bounding boxes per phrase, addressing the core limitations of prior approaches.
- We release a weakly annotated dataset for GMPG pre-training called **GMPG-ImaGenome**, created through an LLM-assisted weak-annotation cleanup pipeline for Chest ImaGenome that removes redundant anatomical regions, filters negative sentences with spurious boxes, and adds explicit non-grounding examples.
- We propose **MedGrounder**, the first GMPG model, which uses a data-efficient two-stage (weak-to-expert) training strategy to achieve state-of-the-art performance on the PadChest-GR and MS-CXR benchmarks, especially on multi-region and non-groundable phrases.
- We demonstrate a **modular, data-efficient approach to grounded report generation**, showing that MedGrounder can be composed with existing text generators to achieve results competitive with end-to-end GRG model while using far fewer human-annotated boxes.
- All code, models, and data-processing scripts will be made publicly available at <https://github.com/Claire1217/MedGrounder>.

II. RELATED WORK

We review literature across three domains: MPG, REC (and GREC), and GRG, with methods summarised in Table I

A. Medical phrase grounding (MPG)

1) *Without box supervision*: Initial approaches to MPG did not rely on box supervision, learning local alignments from image-text pairs without explicit bounding box annotations. Contrastive learning models like GLoRIA [12], BioViL [8] and BioViL-T [13] exemplify this; they naturally produce heatmaps from their alignment scores. The MS-CXR benchmark [8] was, in fact, introduced to evaluate this emergent localisation capability against ground-truth boxes, rather than as a primary training set for grounding models. More recently, latent diffusion models [14], [15] have been used to extract cross-attention maps for zero-shot localisation. While these methods offer a way to learn alignments without expensive box annotations, their reliance on coarse heatmaps often limits localisation precision.

2) *With box supervision*: Methods trained with box supervision typically achieve higher precision than the previously mentioned non-box-supervised approaches. MedRPG pioneered this approach by formally defining the MPG task [2]. It was also the first to use the MS-CXR benchmark for training explicit box predictors, rather than solely for evaluation. MedRPG adapted the REC-style TransVG model for medical images, introducing the TaCo module to strengthen region-phrase alignment. AGPT extended this approach by adding an anatomical pretraining stage on anatomy name-box pairs before fine-tuning on expert-annotated sentence-level data [1]. However, these methods all share a fundamental limitation: they adopt the traditional REC framework, which constrains them to predict exactly one bounding box per phrase. Consequently, they are trained on single-box subsets of datasets and cannot handle multi-region findings or non-groundable phrases.

Subsequent work has attempted to address parts of this limitation. MedRG [16] reframed the task as medical report grounding to handle non-groundable text. This multi-stage approach first uses a fine-tuned language model to extract a single, supposedly groundable phrase from a full report, which a separate decoder then grounds. While this adds a mechanism to filter some non-groundable phrases, it introduces architectural complexity and, critically, retains the single-box

constraint, failing to support multi-region findings.

Beyond REC, other methods couple grounding with different objectives. ChEX [17] introduced a model based on DETR [18] for interactive localisation and region description, which is capable of predicting multiple boxes with confidence scores. VG-CT [19] proposed a model that outputs segmentation masks from text, given an image and anatomical segmentation priors. However, none of the existing MPG methods satisfies all three core requirements for GMPG: multi-region support, groundability, and confidence scoring.

B. Referring expression comprehension (REC) and its generalisation

The single-box constraint observed in MPG stems from the adoption of the traditional REC framework in general domain. Traditional REC tasks assumes every textual expression refers to exactly one object in the image. This assumption is embedded in benchmark datasets like ReferIt and RefCOCO(g) [20]–[22], which contain only groundable phrases with single corresponding bounding box. Architecturally, REC-styled models regress directly on four bounding box coordinates without producing confidence scores, making single-box prediction intrinsic to their design.

This limitation led to GREC, which reframes grounding as set prediction: predict a variable-sized set of bounding boxes—including zero when appropriate [4], [23]. Detection Transformers like MDETR enable this by treating grounding as set prediction with cross-modal fusion and learnable object queries, naturally handling zero-or-more outputs with confidence scores [6]. Our work systematically adapts this more flexible formulation to medical imaging.

C. Grounded report generation (GRG)

Radiology report generation aims to automatically produce a free-text radiology report from an input image (or image series) [24]–[29]. GRG extends this setting by producing a report while simultaneously localising the described findings [11], [30], [31]. After each sentence is generated, the model typically outputs the corresponding bounding boxes that indicate the image regions supporting that sentence. GRG is closely related to GMPG, as it inherently involves phrase grounding as a subtask. Consequently, a GMPG model can be combined with an existing report generator to achieve GRG functionality, without the need for additional GRG-specific training.

MAIRA-2 [11] is the current state-of-the-art grounded report generation model we compare against. It accomplishes this by converting spatial coordinates into discrete spatial tokens. MAIRA-2 is trained in three modes aligned with three tasks: findings generation (FG), grounded report (GR), and phrase grounding (PG). The authors build task-specific instruction prompts and train each mode on different datasets. Notably, MAIRA-2 relies on training on large-scale, non-public datasets of image-sentence-box annotations.

III. METHODOLOGY

A. Generalised medical phrase grounding

We define GMPG as mapping a medical image and a phrase to a *set of regions*. Let the dataset be:

$$\mathcal{D} = \{(I_m, \mathcal{P}_m, \{S_{mi}\}_{i=1}^{N_m})\}_{m=1}^M, \quad (1)$$

consisting of M image-report pairs, where I_m denotes the image and $\mathcal{P}_m = \{p_{mi}\}_{i=1}^{N_m}$ denotes its report. $\{S_{mi}\}_{i=1}^{N_m}$ represents the ground-truth bounding-box sets, defined as $S_{mi} = \{b_{mij}\}_{j=1}^{K_{mi}}$, where $b_{mij} \in [0, 1]^4$ is a normalised box and $K_{mi} \geq 0$ is the region count. GMPG maps a pair (I, p) to a predicted set $\hat{S}_{mi} = f(I_m, p_{mi})$ approximating S_{mi} . The variable cardinality K_{mi} supports multi-box grounding and non-groundable phrases, expanding upon MPG which assumes $|S_{mi}| = 1$.

B. MedGrounder framework

MedGrounder builds upon the MDETR framework [6] (Fig. 2). The image I is encoded by ResNet-101 [32] and the phrase p by BioClinical ModernBERT [33]. A cross-modal encoder fuses features for a Transformer decoder, which outputs N_Q queries. Each query passes through a box FFN (coordinates) and a confidence FFN (linear projection).

For each pair (I_m, p_{mi}) , the model predicts $\hat{Y} = \{(\hat{b}_j, \hat{c}_j)\}_{j=1}^{N_Q}$ (indices dropped for clarity). We compute a one-to-one assignment $\hat{\pi}$ by minimising the matching cost:

$$\hat{\pi} = \arg \min_{\pi} \sum_{k=1}^K \left[-\hat{c}_{\pi(k)} + \lambda_{L1} \|\hat{b}_{\pi(k)} - b_k\|_1 + \lambda_{\text{giou}} \mathcal{L}_{\text{giou}} \right], \quad (2)$$

where $\mathcal{L}_{\text{giou}} = 1 - \text{GIoU}(\hat{b}_{\pi(k)}, b_k)$. We define binary targets $t_j = 1$ if matched, else 0. The groundability (\mathcal{L}_{cls}) and localisation (\mathcal{L}_{box}) objectives are:

$$\mathcal{L}_{\text{cls}} = (1/N_Q) \sum_{j=1}^{N_Q} \alpha_{t_j} \text{BCE}(\hat{c}_j, t_j), \quad (3)$$

$$\mathcal{L}_{\text{box}} = \frac{1}{\max(1, K)} \sum_{k=1}^K (\lambda_{L1} \|\hat{b}_{\hat{\pi}(k)} - b_k\|_1 + \lambda_{\text{giou}} [1 - \text{GIoU}(\hat{b}_{\hat{\pi}(k)}, b_k)]). \quad (4)$$

Total loss is $\mathcal{L} = \mathcal{L}_{\text{cls}} + \mathcal{L}_{\text{box}}$, where we set $\alpha_{t_j=0} = 0.1$, $\lambda_{L1} = 5$, and $\lambda_{\text{giou}} = 2$.

C. Datasets

Our experiments utilize three chest X-ray datasets containing image-sentence-box pairs: Chest ImaGenome, PadChest-GR, and MS-CXR. Table II summarizes their key statistics.

Chest ImaGenome [7], built on MIMIC-CXR [34], is used in our pipeline by taking each report sentence together with the anatomical bounding boxes assigned to that sentence (covering 29 predefined regions). This dataset offers large-scale coverage across diverse disease types and sentence structures, providing rich variability. Because the boxes are automatically generated rather than expert-verified, we treat them as weak supervision. We use a large language model to perform dataset cleaning to reduce noisy, overlapping, or redundant annotations. The

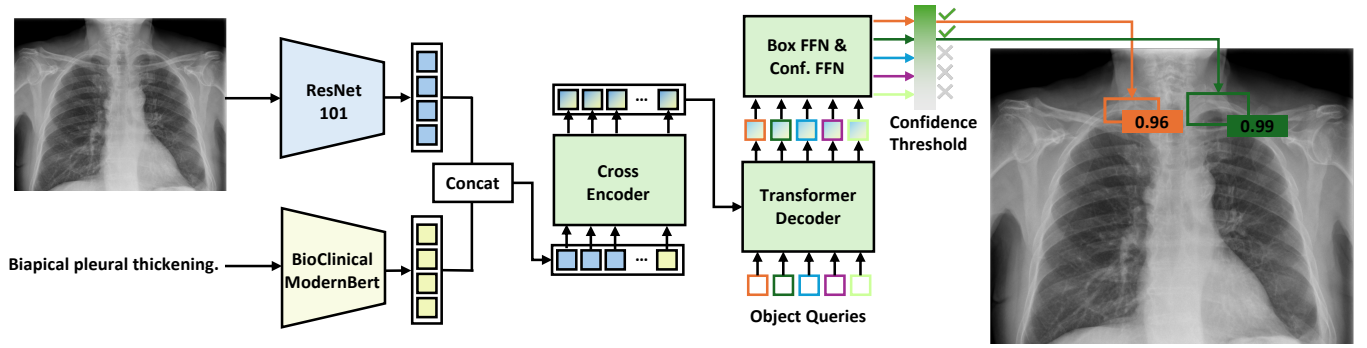


Fig. 2. MedGrounder architecture overview. ResNet-101 and BioClinical ModernBERT encode image and phrase features, respectively, which are concatenated and fed into a cross-encoder. From the features of the cross-encoder, a Transformer decoder then predicts a set of scored bounding boxes corresponding to the phrase, with an example shown on the right.

TABLE II

STATISTICS OF DATASETS FOR PRETRAINING AND FINE-TUNING OF MEDGROUNDER. THE TABLE DETAILS THE PROPOSE, SPLITS, SIZES, AND ANNOTATION CHARACTERISTICS OF CHEST IMAGENOME, PADCHEST-GR, AND MS-CXR.

Dataset	Purpose	Annotation source	Region type	Split	#Image	#Image-phrase	#Boxes	#Boxes per phrase (%)	Sent. length Mean \pm SD
Chest ImaGenome	Pretraining	Model generated	Anatomy	train	137 065	764 540	426 749	64 / 19 / 17	9.2 \pm 5.8
PadChest-GR	Fine-tuning	Human labeled	Pathology	train	3 185	7 310	5 404	41 / 46 / 13	5.1 \pm 3.2
				val	455	1 052	808	39 / 46 / 14	5.2 \pm 3.6
				test	915	2 112	1 521	41 / 47 / 12	5.3 \pm 3.5
MS-CXR	Fine-tuning	Human labeled	Pathology	train	737	815	1 020	0 / 77 / 23	5.7 \pm 3.5
				val	155	169	212	0 / 76 / 24	5.9 \pm 3.4
				test	155	176	216	0 / 78 / 22	5.5 \pm 3.3

cleaned split is used in the first stage of training, detailed in Subsection III-D.1.

PadChest-GR [9] and **MS-CXR** [8] are smaller, expert-annotated datasets used primarily for fine-tuning and evaluation. In contrast to Chest ImaGenome, they consist of shorter, more focused text spans. PadChest-GR contains English translations of Spanish report sentences, while MS-CXR includes concise phrases extracted from approximately one thousand MIMIC-CXR reports. All three datasets permit multi-box annotations, with multi-box rates of 17% in Chest ImaGenome, 12–14% in PadChest-GR, and 22–24% in MS-CXR. Zero-box cases are common in Chest ImaGenome and present in PadChest-GR but absent in MS-CXR.

D. Training Strategy

1) *Weak annotations cleanup*: Chest ImaGenome provides sentence-level grounding by aligning radiology report sentences from MIMIC-CXR with anatomical bounding boxes. However, the original annotations contain notable noise. Sentences are often linked to both specific and overly broad anatomical regions (for example, “right lower lung zone” together with “right lung”), reducing spatial precision. Furthermore, sentences describing normal findings (for example, “No focal consolidation, pleural effusion, or pneumothorax”) are still assigned bounding boxes, introducing false positive sentence–region pairs.

We applied a three-stage cleaning procedure to improve supervision quality. First, we used LLaMA-3-70B [35] to retain only the most specific regions associated with each sentence

LLM Prompt for Region Filtering

System: Given a radiology report sentence and its candidate anatomical regions, return only the most specific regions that correspond to the described abnormality. Remove broader or redundant regions. Output valid JSON with the key “selected_region” only.

User: Sentence: “There is minimal upper zone vascular redistribution without overt pulmonary edema.”
Candidates: [“right lung”, “right upper lung zone”, “right hilar structures”, “left lung”, “left upper lung zone”, “left hilar structures”]

Expected output: {“selected_regions”: [“right upper lung zone”, “left upper lung zone”]}

Fig. 3. LLM prompt for filtering redundant anatomical regions. The model selects the most specific regions from candidates, discarding broader parent regions.

and discard redundant parent regions. The prompt used for this filtering step is shown in Figure 3. Second, we removed all anatomical regions associated with sentences containing only negative findings, ensuring the model learns to produce no box when appropriate. Third, we added report sentences that were not mapped to any anatomical regions in the original dataset (for example, “PA views of the chest obtained.”), providing additional non-grounding cases. To prevent data leakage, we further excluded all studies overlapping with MS-CXR. Overall, these steps reduced the dataset by 89.6%, from more than four million to 426 749 sentence–box pairs.

2) *Multi-stage training*: We adopt a two-stage training pipeline. In stage one, the model is pretrained on weak annotations from the cleaned Chest ImaGenome to learn broad anatomical regions that radiology reports are describing. In stage two, we further fine-tune on the expert-annotated MS-

CXR and PadChest-GR to ground exact pathological regions.

E. Evaluation Metrics for GMPG

REC-style metrics, such as mIoU and mIoU accuracy, are not sufficient for GMPG, since phrases may map to zero, one, or multiple boxes. We therefore report Precision@($F_1=1$, $\text{IoU} \geq 0.5$) and Negative Accuracy (N-Acc) following [4], as well as Center-Hit F1 (CH-F1), and Mask IoU accuracy. Precision@($F_1=1$) strictly rewards exact set matches and penalises extra boxes; N-Acc measures correct abstention on non-groundable phrases; CH-F1 relaxes boundary sensitivity by requiring predicted box centres to fall inside the ground-truth region; Mask IoU measures the intersection over union of pixel masks for all matched predicted and ground-truth boxes across images; Mask IoU accuracy is the proportion of predictions whose mask IoU is at least 0.5.

F. Evaluation Metrics for Grounded Report Generation

For grounded report generation, we adopt the RadFact evaluation framework introduced in MAIRA-2 [11]. RadFact leverages large language models to assess report quality at the sentence level through three hierarchical metrics: (i) *logical F1* measures whether generated sentences are factually entailed by the ground-truth report; (ii) *grounding F1* evaluates whether logically correct sentences are also spatially entailed; and (iii) *spatial F1* measures the fraction of all grounded sentences that are both logically and spatially correct.

IV. EXPERIMENT SETUP

1) *Data preparation*: Following MedRPG, each image was resized so that its longer side was 640 pixels while preserving aspect ratio, then zero-padded to a 640×640 square. Training time image augmentations included Gaussian noise and random cropping. Images were normalised with ImageNet mean and standard deviation, following DETR. Boxes were transformed with the images, and any with less than 90% visibility after augmentation were discarded.

2) *Training and inference setup*: MedGrounder was first pretrained on the cleaned Chest ImaGenome for 15 epochs (batch size 32) using AdamW [36] with a $1e-5$ learning rate; the checkpoint with the best validation Mask IoU was kept for fine-tuning. In stage two, we fine-tuned on PadChest-GR and MS-CXR for 15 epochs with the same settings, selecting the final model by the much stricter metric $P@F_1=1$. All runs used a single NVIDIA H100 96GB GPU. At inference time, predictions were filtered by an optimised confidence threshold and merged with weighted box fusion (WBF).

3) *Baselines*: We compared MedGrounder against state-of-the-art models in two distinct tasks.

a) *GMPG*: We benchmarked against two families of box-supervised baselines. The first was REC-style models, which included TransVG, MedRPG, and AGPT. The second was GRG models, for which we compared against MAIRA-2. To ensure a fair comparison, all models were evaluated on the official MS-CXR split; MedRPG and AGPT were retrained accordingly. Furthermore, MAIRA-2 was evaluated in both

phrase-grounding (PG) and grounded-report (GR) modes, as its original training was split by mode (PadChest-GR for GR and MS-CXR for PG).

b) *GRG*: To evaluate MedGrounder for GRG, we compared an end-to-end grounded report generation model (MAIRA-2 GR) with two pipeline approaches: MAIRA-2 FG + MedGrounder and CXRMate-RRG24 [37] + MedGrounder. Because the training data for CXRMate-RRG24 (the original PadChest) overlaps with the PadChest-GR test set, we created a 38-case non-overlapping subset to ensure a fair evaluation of all three models.

V. RESULTS & DISCUSSION

A. GMPG evaluation

1) *Main results on Padchest-GR and MS-CXR*: We evaluated MedGrounder's GMPG performance in two settings, presented in Tables III (PadChest-GR) and IV (MS-CXR): zero-shot generalisation (Panel A) and in-domain fine-tuning (Panel B). The results reveal two key findings.

Finding 1: MedGrounder exhibits superior zero-shot generalisation. Panel A of both tables highlights the effectiveness of our pretraining strategy. Without exposure to any samples from PadChest-GR or MS-CXR, MedGrounder achieved the highest scores across all metrics. These results indicate that pretraining on sentence-anatomical region alignments provides a significantly stronger inductive bias than aligning anatomical regions with anatomy names alone, which was used as pretraining strategy in AGPT [1]. In contrast, models such as MedRPG trained on MS-CXR transfer poorly to PadChest-GR, underscoring their limited cross-dataset generalisation capability.

Finding 2: MedGrounder achieves state-of-the-art performance, particularly on multi-box phrases. In the fine-tuned setting (Panel B), MedGrounder consistently outperforms all baselines. While REC-style models remain competitive on single-box phrases, MedGrounder's advantage is most pronounced on the more challenging multi-box cases. In Table III, it achieves 28.6% $P@F_1=1$ on multi-box phrases in PadChest-GR, nearly double the score of the strongest competitor MAIRA-2, even though MAIRA-2 GR was trained on roughly ten times more human-annotated data. Likewise, on MS-CXR (Table IV), MedGrounder pretrained on Chest ImaGenome and fine-tuned exclusively on MS-CXR establishes a new state-of-the-art across all multi-box metrics and overall performance.

2) *Qualitative analysis on Padchest-GR*: Figure 4 presents qualitative comparisons on the PadChest-GR test set. The first example has three sentences, two requiring multi-box localisation and one requiring a single box. The MPG models output only a single box per phrase, failing at multi-region grounding. By contrast, MAIRA-2 GR and MedGrounder correctly localise multiple regions. In the second and third examples, phrases such as "No significant findings" are not groundable. The MPG models still output a box, whereas MAIRA-2 GR and MedGrounder correctly skip these phrases, yielding N-ACC = 1. Across all cases, MedGrounder handles non-groundable and multi-box phrases, provides per-phrase confidence scores, and attains the highest Mask IoU.

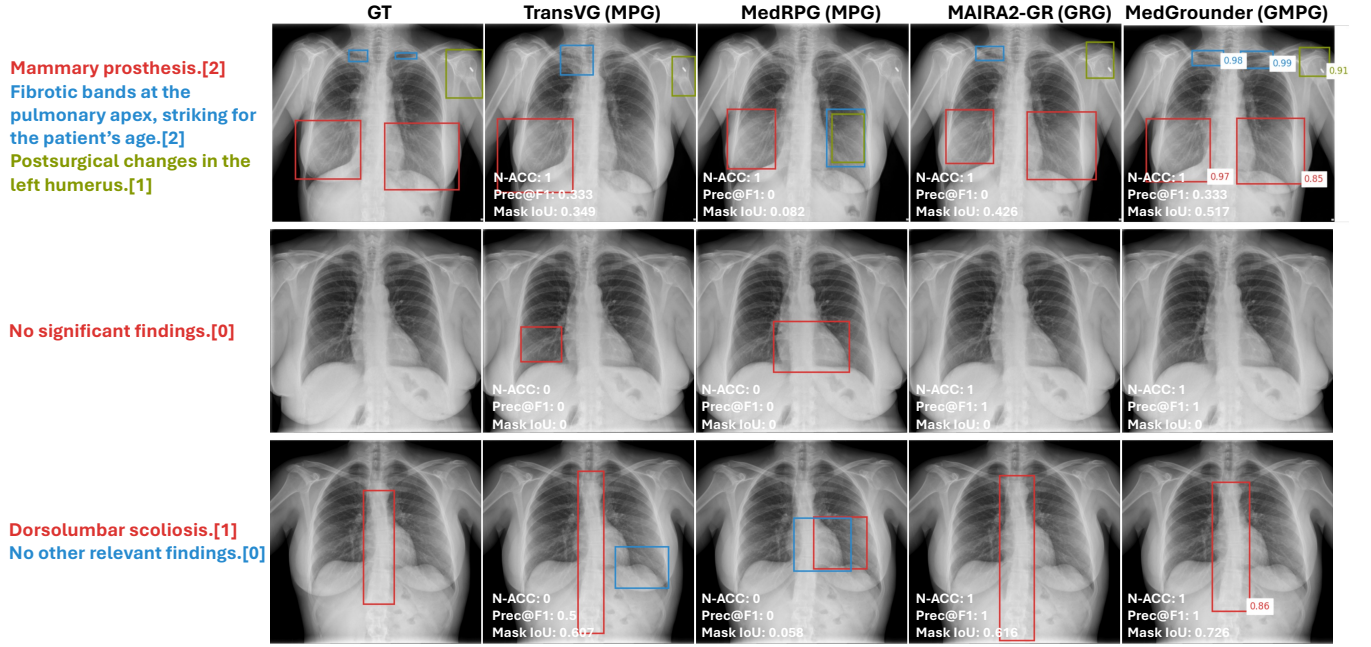


Fig. 4. Qualitative comparison of grounding results from TransVG, MedRPG, MAIRA-2 GR, and the proposed MedGrounder on three PadChest-GR examples. Ground-truth (GT) is shown in the first column, model predictions in the remaining columns. Numbers in brackets after each sentence indicate the number of bounding boxes in the GT.

TABLE III

PHRASE GROUNDING PERFORMANCE ON THE TEST SET OF PADCHEST-GR. MODELS ARE GROUPED INTO (A) MODELS NOT TRAINED ON PADCHEST-GR AND (B) MODELS TRAINED OR FINE-TUNED ON PADCHEST-GR. BEST RESULTS ARE **BOLD**, SECOND BEST ARE UNDERLINED.

Model	Supervision			No (<i>n</i> = 874)	Single (<i>n</i> = 983)			Multi (<i>n</i> = 255)			Overall (<i>n</i> = 2 112)		
	Framework	Datasets	Annots.	N-Acc	P@F1=1	CH-F1	Acc	P@F1=1	CH-F1	Acc	P@F1=1	CH-F1	Acc
(A) Models not trained on PadChest-GR													
MedRPG	MPG	M*	624	<u>0</u>	<u>13.2</u>	35.4	12.7	<u>0</u>	34.9	<u>0.8</u>	<u>6.2</u>	25.9	<u>10.3</u>
AGPT (pretrained)	MPG	–	0	<u>0</u>	13.0	39.9	12.9	<u>0</u>	37.4	0	6.1	29.6	<u>10.3</u>
MedGrounder (pretrained)	GMPG	–	0	86.5	18.1	60.2	21.2	8.2	65.3	16.1	45.2	58.2	20.1
(B) Models trained on PadChest-GR													
TransVG	MPG	M*,P*	3 993	0	54.4	82.6	54.2	0	56.8	5.1	25.3	56.0	44.1
MAIRA-2 PG	GRG	U,M,P	73 043	72.1	39.6	74.4	40.8	14.9	73.1	26.7	50.0	66.1	37.9
MAIRA-2 GR	GRG	U,M,P	73 043	91.0	45.8	<u>79.5</u>	47.0	14.9	74.1	31.8	60.7	75.1	43.9
MedGrounder	GMPG	P	7 315	88.1	47.5	77.1	48.8	<u>21.6</u>	76.7	<u>34.5</u>	<u>61.2</u>	73.3	45.9
MedGrounder	GMPG	M,P	8 130	<u>90.1</u>	<u>47.7</u>	77.2	<u>49.8</u>	28.6	78.3	37.3	62.9	<u>74.5</u>	47.3

Notes: Datasets: M = MS-CXR, P = PadChest-GR, U = US-Mix. Annots. is the number of human-annotated phrases used during training; Annots. = 0 means the model used only non human-annotated weak labels. Dataset names with an asterisk (M*, P*) indicate that only the single-box portions were used.

TABLE IV

GROUNDING PERFORMANCE ON THE TEST SET OF MS-CXR. MODELS ARE GROUPED INTO (A) MODELS NOT TRAINED ON MS-CXR AND (B) MODELS TRAINED OR FINE-TUNED ON MS-CXR.

Model	Supervision			Single (n = 138)			Multi (n = 38)			Overall (n = 176)		
	Framework	Datasets	Annots.	P@F1=1	CH-F1	Acc	P@F1=1	CH-F1	Acc	P@F1=1	CH-F1	Acc
(A) Models not trained on MS-CXR												
AGPT(pretrained)	MPG	–	0	<u>29.7</u>	<u>60.9</u>	<u>29.0</u>	<u>0.0</u>	<u>14.8</u>	<u>0.0</u>	<u>23.3</u>	<u>47.6</u>	<u>22.7</u>
MedGrounder(pretrained)	GMPG	–	0	43.5	78.7	45.7	13.2	81.5	18.4	36.9	79.9	39.8
(B) Models trained on MS-CXR												
TransVG	MPG	M*,P*	3993	<u>71.7</u>	94.6	<u>71.0</u>	0.0	59.0	7.9	56.2	83.8	57.4
MedRPG	MPG	M*	624	<u>71.7</u>	93.4	73.9	0.0	54.0	2.6	56.2	81.6	58.5
AGPT	MPG	M*	624	73.2	90.8	73.9	0.0	50.7	5.3	<u>57.4</u>	78.7	<u>59.1</u>
MAIRA-2 PG	GRG	U,M,P	73043	55.8	91.2	55.1	26.3	81.5	<u>36.8</u>	49.4	88.0	51.1
MAIRA-2 GR	GRG	U,M,P	73043	50.7	86.6	52.2	0.0	18.9	15.8	39.8	77.0	44.3
MedGrounder	GMPG	M	815	67.4	90.9	68.8	26.3	85.2	42.1	58.5	88.9	63.1
MedGrounder	GMPG	M,P	8130	60.1	86.7	61.6	<u>21.1</u>	<u>82.5</u>	28.9	51.7	85.2	54.5

TABLE V

DISEASE-SPECIFIC PERFORMANCE AND TRAINING DATA CHARACTERISTICS ON MS-CXR. PERFORMANCE REPORTED AS PERCENTAGES (ONE DECIMAL PLACE); COUNTS N UNCHANGED. ROWS ORDERED BY DESCENDING P@F1.

Disease Name	Performance Metrics (%)			Training Data Characteristics		
	P@F1=1	CH-F1	mIoU	N	Avg. Area (%)	SDS (%)
Cardiomegaly	100.0	100.0	78.3	232	17.2	9.4
Atelectasis	62.5	96.0	51.0	72	5.8	25.7
Pleural Effusion	50.0	95.0	51.4	97	5.5	29.9
Pneumonia	46.7	86.0	46.8	163	7.5	25.4
Consolidation	40.0	90.9	47.6	138	7.3	27.5
Pneumothorax	38.9	74.7	45.3	182	5.0	27.5
Edema	25.0	82.8	41.6	61	11.5	25.3
Lung Opacity	16.7	73.0	34.4	75	6.4	27.7

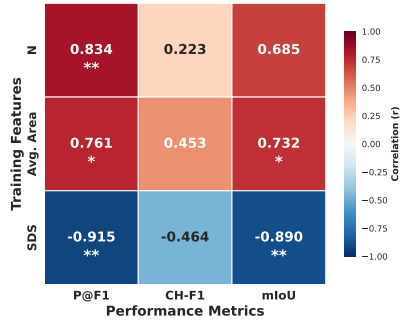


Fig. 5. **Correlation heatmap on MS-CXR.** Performance vs. data properties; cell text shows Pearson r and p -values. Asterisks indicate statistical significance levels, ** $p < 0.01$, and * $p < 0.05$.

3) *Disease specific analysis on MS-CXR:* Table V shows that MedGrounder’s performance depends strongly on disease characteristics. Anatomically constrained findings such as cardiomegaly are localised with near-perfect accuracy, whereas performance drops for diffuse, small, or highly variable findings such as lung opacity and edema. CH-F1 remains high across most pathologies, indicating that the model usually identifies the correct general location. In contrast, the larger variation in mIoU suggests that precisely capturing lesion extent is harder, especially for diffuse or irregular cases.

The correlation analysis in Figure 5 quantifies these effects. Performance improves with more samples and larger average box area, but the strongest predictor is the Spatial Dispersion Score (SDS), which is strongly negatively correlated with both P@F1 and mIoU. Thus, findings with high anatomical variability i.e., those that may appear in many different locations, exhibit the largest drop in localisation accuracy. A plausible explanation is that Chest ImaGenome does not provide meaningful supervision for spatially variable or diffuse findings. Its rule-based annotations map sentences only to fixed anatomical regions, which is adequate for findings with consistent anatomical location but offers no region-level guidance for abnormalities that can arise across diverse lung regions. As a result, the model enters fine-tuning with weaker spatial priors for these findings, contributing to the drop in localisation performance when such findings do appear in the expert-annotated downstream datasets.

4) *Disease specific case studies on MS-CXR and PadChest-GR:* Figure 6 visualises MedGrounder’s performance on the MS-CXR test set, highlighting correct ($\text{Mask IoU} \geq 0.5$) and error cases. The model performs well when phrases contain explicit spatial cues (e.g., “bibasilar” and “left lower lung”), while phrases lacking clear anatomical indicators like “pulmonary edema” or “side-unspecified apical pneumothorax” sometimes leads to errors. For diffuse findings such as “pleural effusion”, predictions sometimes target the correct region even when Mask IoU is below 0.5.

On the PadChest-GR test set (Figure 7), we observe similar trends. High-performing findings are tightly linked to specific anatomies (e.g., “cardiomegaly”, “aortic elongation”, “costophrenic angle blunting”), where anatomical priors suffice for accurate localisation. The worst-performing findings either have inconsistent ground-truth boxes (e.g., “chronic changes”, “air trapping”) or high spatial variance (e.g., “calcified granuloma”, “nodule”, “rib fracture”), where the model often resorts to multiple speculative boxes.

B. MedGrounder for grounded report generation

TABLE VI

RADFACT EVALUATION ON PADCHEST-GR. WE REPORT METRICS ON THE FULL SET ($n = 915$) AND A NON-OVERLAPPING SUBSET ($n = 38$). CXRMate-RRG24 IS EVALUATED ONLY ON THE SUBSET TO AVOID TRAINING DATA OVERLAP.

Model	Set	Logical	Grounding	Spatial
MAIRA-2 GR	Full	53.89	77.63	27.92
MAIRA-2 FG + MedGrounder	Full	53.69	75.41	28.17
MAIRA-2 GR	Subset	70.91	89.89	52.03
MAIRA-2 FG + MedGrounder	Subset	69.21	95.45	53.52
CXRMate-RRG24 + MedGrounder	Subset	65.75	97.14	41.58

To evaluate MedGrounder’s ability to ground model-generated reports, we compared an end-to-end baseline (MAIRA-2 GR) with two pipeline approaches that first generate text and then apply MedGrounder for localisation: MAIRA-2 in finding-generation mode (MAIRA-2 FG) and CXRMate-RRG24. For MAIRA-2 GR and MAIRA-2 FG + MedGrounder, we report results on the full PadChest-GR test set. Since CXRMate-RRG24 was trained on PadChest, which overlaps with the PadChest-GR test set, we removed the overlaps and formed a 38-case subset for fair evaluation. We report results on this subset for all three models.

Table VI demonstrates that grounding the generated reports of MAIRA-2 FG or CXRMate-RRG24 with MedGrounder performs on par with MAIRA-2 GR. In particular, MAIRA-2 FG + MedGrounder achieved the highest Spatial F1 on both sets, while CXRMate-RRG24 + MedGrounder achieved the highest Grounding F1 on the subset. This is notable given the training regimes: MAIRA-2 models are trained on US-MIX, a private dataset with human bounding-box annotations; MedGrounder is trained on one tenth of the number of human annotations. Together, the results indicate that MedGrounder enables modular GRG that can match—or exceed—a specialised end-to-end system, while avoiding having to train grounded report generator.

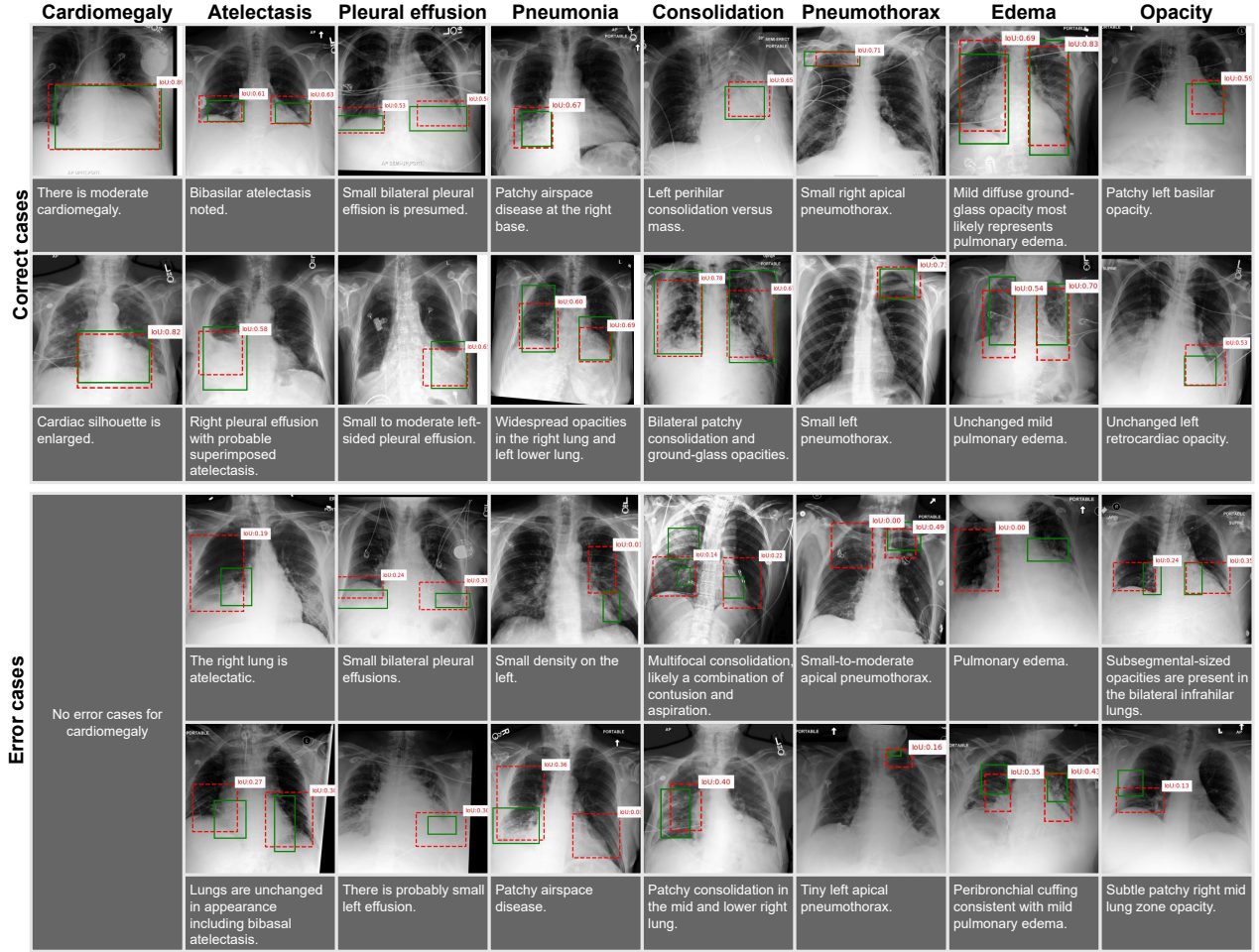


Fig. 6. Visualisation result of our model on MS-CXR across eight findings. Ground truth boxes are green, model predictions are red (dashed) with IoU shown. Top: correct cases. Bottom: error cases for the same disease; no cardiomegaly error example appears.

C. Ablation Studies

We conducted a series of ablation studies to validate the impact of our key design choices: the two-stage training strategy, post-processing pipelines including confidence thresholding and weighted box fusion, and the in-domain language encoder.

TABLE VII

MEDGROUNDER PRETRAINING AND FINE-TUNING STRATEGY ABLATION.

Training regime	MS-CXR				PadChest-GR			
	P@F1=1	CH-F1	mIoU	P@F1=1	CH-F1	mIoU	N-Acc	
Padchest-GR (from scratch)	0	0	8.1	41.3	1.5	8.9	99.8	
MS-CXR (from scratch)	0	4.7	22.0	41.3	2.9	24.9	99.9	
Pretrain→Zero Shot	36.9	79.9	42.7	45.2	58.2	32.3	86.5	
Pretrain→FT PadGR	42.0	80.7	47.9	57.7	70.8	44.4	82.6	
Pretrain→FT MS-CXR	58.5	88.4	55.8	44.0	56.5	32.2	84.7	
Pretrain→FT PadGR+MS-CXR	54.0	86.7	54.1	61.3	73.2	46.8	85.7	

1) *Impact of pretraining and fine-tuning stage*: Our ablation study on training strategy, presented in Table VII, shows three key findings. First, pretraining is essential for GMPG, as training from scratch on either MS-CXR or PadChest-GR fails

to produce meaningful results, with center-hit scores near zero. Second, by pre-training on our cleaned Chest Imagenome, our MedGrounder achieves respectable zero-shot performance on both datasets. Finally, fine-tuning a pretrained model further boosts performance, with the optimal strategy depending on the target dataset. Fine-tuning solely on MS-CXR yielded the best results on MS-CXR, while fine-tuning on a combination of both datasets was best for PadChest-GR.

TABLE VIII

MEDGROUNDER POST-PROCESSING ABLATION: WEIGHTED BOXES FUSION (WBF) ENABLED VS DISABLED

Post-processing	MS-CXR				PadChest-GR			
	P@F1=1	CH-F1	mIoU	P@F1=1	CH-F1	mIoU	N-Acc	
without WBF (baseline)	44.3	86.8	55.1	57.9	75.6	48.5	90.1	
with WBF	51.7	85.2	54.5	62.9	74.5	47.3	90.1	

2) *Impact of post-processing*: We select the confidence threshold by analysing center-hit precision–recall on the validation sets of MS-CXR and Padchest-GR; F1 peaks at 0.8 for both, so we adopt 0.8 throughout. Applying Weighted Box

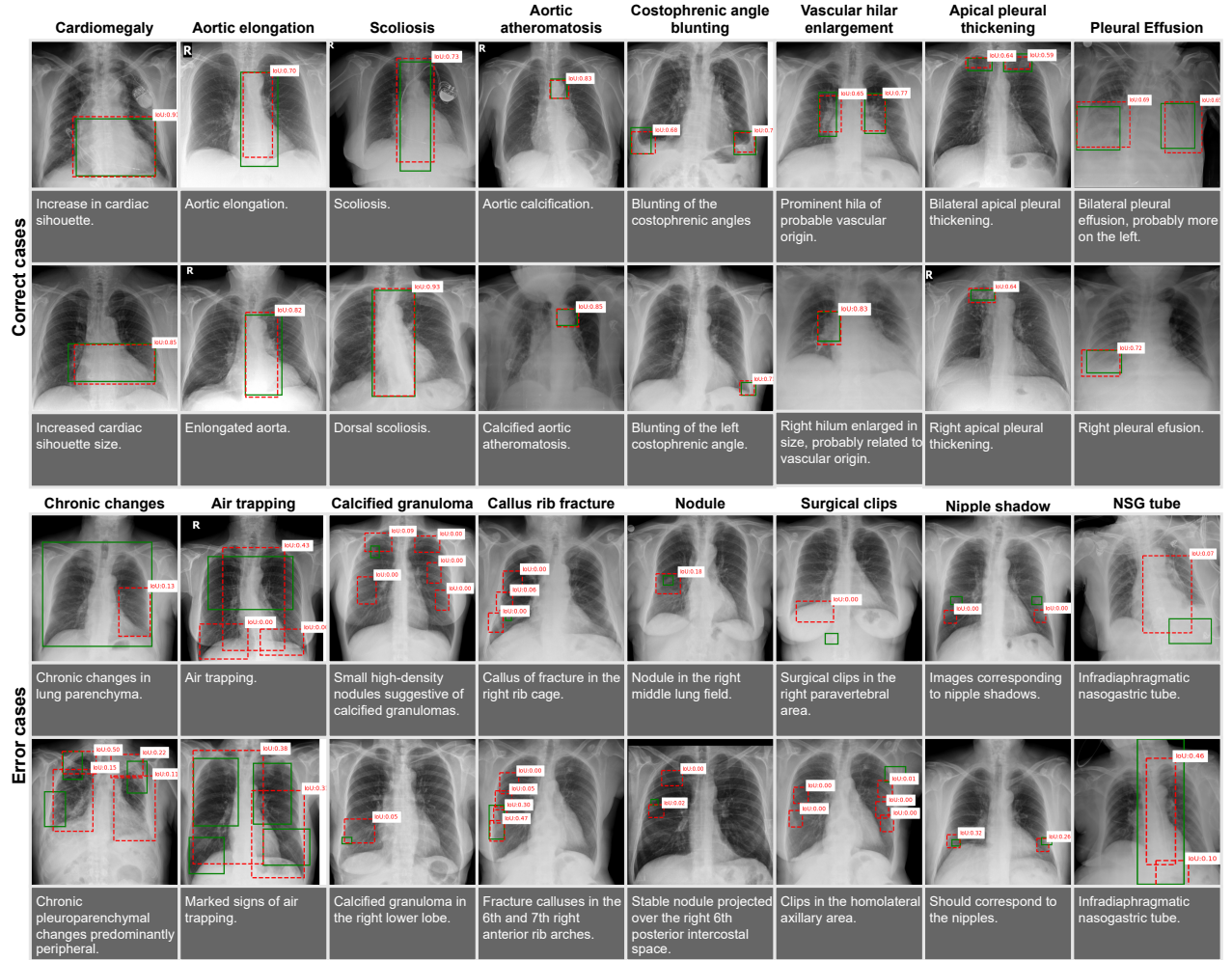


Fig. 7. Visualisation result of our model on PadChest-GR across sixteen findings. The top two rows show eight disease categories with strong phrase grounding results. The bottom two rows show eight categories with weaker performance. Ground-truth regions are green; predicted boxes are red (dashed) with IoU indicated.

Fusion (WBF) with a 0.1 IoU threshold to merge redundant detections further improves performance, raising $P@F1=1$ by +7.4 on MS-CXR and +5.0 on PadChest-GR (Table VIII).

TABLE IX
MEDGROUNDER LANGUAGE ENCODER ABLATION

Model	MS-CXR			PadChest-GR			
	$P@F1=1$	CH-F1	mIoU	$P@F1=1$	CH-F1	mIoU	N-Acc
RoBERTa (baseline)	29.5	78.4	38.1	44.7	57.4	19.9	85.0
ClinicalBERT	35.8	78.9	38.6	45.1	56.5	18.9	86.6
BioClinical ModernBERT	36.9	79.9	42.7	45.2	58.2	32.3	86.5

3) *Impact of In-Domain Language Encoder*: Table IX shows that swapping RoBERTa encoder for a medical-domain model significantly improved performance. The top-performing encoder, BioClinical ModernBERT, boosted the $P@F1=1$ score by +7.4 on MS-CXR and mIoU by +12.4 on PadChest-GR, confirming that in-domain clinical knowledge is crucial for maximising GMPG performance.

VI. CONCLUSION

We introduced generalised medical phrase grounding (GMPG), a new task formulation that addresses fundamental limitations of prior methods by supporting the mapping of findings to zero, one, or multiple image regions. MedGrounder—the first GMPG model—achieves state-of-the-art performance through pretraining on weakly supervised anatomical data (Chest Imagenome) and fine-tuning on small expert-annotated datasets (PadChest-GR, MS-CXR). We also demonstrated MedGrounder’s practical utility as a modular component. By composing our model with existing report generators, we can produce grounded reports with performance competitive with end-to-end systems, offering a scalable path toward verifiable generated reports without retraining generators on image-report-box triplets.

Important limitations remain. MedGrounder excels on anatomically constrained findings (e.g., “cardiomegaly”) yet struggles more on spatially variable (e.g., “rib fractures”) or diffuse (e.g., “pulmonary edema”) findings; single-box

performance is only comparable to existing MPG methods, and absolute multi-box performance still leaves room for improvement. Secondly, evaluation is constrained by dataset scarcity, PadChest-GR and MS-CXR contain brief annotations (5-6 words per sentence) that differ substantially from real-world reports (9.2 words per sentence in MIMIC-CXR). To improve performance on spatially diffuse findings, additional expert supervision will be important. One practical direction is to make use of existing object-detection datasets that provide accurate human annotations for diffuse findings. Though there are not sentences, these disease names can serve as grounding phrases, or be converted into short sentence descriptions to better align with the GMPG setting.

Despite these limitations, MedGrounder's generalisation capability opens promising directions: applying the model to generate weakly-supervised annotations for large-scale unannotated datasets, accelerating human annotation workflows, and providing pre-training data for grounded report generation models facing similar data scarcity constraints.

REFERENCES

- [1] W. Zhang, S. S. Chandra, and A. Nicolson, "Anatomical grounding pre-training for medical phrase grounding," in *ISBI*, 2025, pp. 1–5.
- [2] Z. Chen, Y. Zhou, A. Tran, J. Zhao, L. Wan, G. S. K. Ooi, L. T.-E. Cheng, C. H. Thng, X. Xu, Y. Liu, and H. Fu, "Medical phrase grounding with region-phrase context contrastive alignment," in *MICCAI*, 2023, pp. 371–381.
- [3] T. Tanida, P. Müller, G. Kaissis, and D. Rueckert, "Interactive and explainable region-guided radiology report generation," in *CVPR*, 2023, pp. 7433–7442.
- [4] S. He, H. Ding, C. Liu, and X. Jiang, "GREC: Generalized referring expression comprehension," *arXiv:2308.16182 [cs.LG]*, 2023.
- [5] L. Xiao, X. Yang, X. Lan, Y. Wang, and C. Xu, "Towards visual grounding: A survey," *IEEE Transactions on Pattern Analysis and Machine Intelligence*, pp. 1–20, 2025.
- [6] A. Kamath, M. Singh, Y. LeCun, G. Synnaeve, I. Misra, and N. Carion, "MDETR – modulated detection for end-to-end multi-modal understanding," in *ICCV*, 2021, pp. 1760–1770.
- [7] J. T. Wu, N. N. Agu, I. Lourentzou, A. Sharma, J. A. Paguio, J. S. Yao, E. C. Dee, W. Mitchell, S. Kashyap, A. Giovannini, L. A. Celi, and M. Moradi, "Chest ImaGenome dataset for clinical reasoning," in *NeurIPS*, 2021, pp. 1–14.
- [8] B. Boecking, N. Usuyama, S. Bannur, D. C. Castro, A. Schwaighofer, S. Hyland, M. Wetscherek, T. Naumann, A. Nori, J. Alvarez-Valle, H. Poon, and O. Oktay, "Making the most of text semantics to improve biomedical vision-language processing," in *ECCV*, 2022, pp. 1–21.
- [9] D. C. de Castro, A. Bustos, S. Bannur, S. L. Hyland, K. Bouzid, M. T. Wetscherek, M. D. Sánchez-Valverde, L. Jaques-Pérez, L. Pérez-Rodríguez, K. Takeda, J. M. Salinas-Serrano, J. Alvarez-Valle, J. Galant-Herrero, and A. Pertusa, "PadChest-GR: A bilingual chest X-ray dataset for grounded radiology report generation," *NEJM AI*, vol. 2, no. 7, p. 6, 2025.
- [10] N. Yildirim, H. Richardson, and e. a. Wetscherek, "Multimodal healthcare AI: Identifying and designing clinically relevant vision-language applications for radiology," *Conference on Human Factors in Computing Systems - Proceedings*, vol. 22, 2, 2024.
- [11] S. Bannur, K. Bouzid, D. Coelho de Castro, A. Schwaighofer, S. Bond-Taylor, M. Ilse, F. Pérez-García, V. Salvatelli, H. Sharma, F. Meissen, M. Ranjit, S. Srivastav, J. Gong, F. Falck, O. Oktay, A. Thieme, M. P. Lungren, M. T. Wetscherek, J. Alvarez-Valle, and S. Hyland, "MAIRA-2: Grounded radiology report generation," Microsoft, Tech. Rep., 2024.
- [12] S.-C. Huang, L. Shen, M. P. Lungren, and S. Yeung, "GLORIA: A multimodal global-local representation learning framework for label-efficient medical image recognition," in *ICCV*, 2021, pp. 3942–3951.
- [13] S. Bannur, S. Hyland, Q. Liu, F. Perez-Garcia, M. Ilse, D. C. Castro, B. Boecking, H. Sharma, K. Bouzid, A. Thieme, A. Schwaighofer, M. Wetscherek, M. P. Lungren, A. Nori, J. Alvarez-Valle, and O. Oktay, "Learning to exploit temporal structure for biomedical vision-language processing," in *CVPR*, 2023, pp. 15 016–15 027.
- [14] K. Vilouras, P. Sanchez, A. Q. O'neil, and S. A. Tsaftaris, "Zero-shot medical phrase grounding with off-the-shelf diffusion models," *IEEE Journal of Biomedical and Health Informatics*, 2024.
- [15] F. Nützel, M. Dombrowski, and B. Kainz, "Generate to ground: Multimodal text conditioning boosts phrase grounding in medical vision-language models," in *Medical Imaging with Deep Learning*, 2025.
- [16] K. Zou, Y. Bai, Z. Chen, Y. Zhou, Y. Chen, K. Ren, M. Wang, X. Yuan, X. Shen, and H. Fu, "MedRG: Medical report grounding with multi-modal large language model," *arXiv:2404.06798 [cs.CV]*, 2024.
- [17] P. Müller, G. Kaissis, and D. Rueckert, "ChEX: Interactive localization and region description in chest X-rays," in *ECCV*, 2024, pp. 92–111.
- [18] N. Carion, F. Massa, G. Synnaeve, N. Usunier, A. Kirillov, and S. Zagoruyko, "End-to-end object detection with transformers," in *ECCV*, 2020, pp. 213–229.
- [19] A. Ichinose, T. Hatsutani, K. Nakamura, Y. Kitamura, S. Iizuka, E. Simo-Serra, S. Kido, and N. Tomiyama, "Visual grounding of whole radiology reports for 3D CT images," in *MICCAI*, 2023, pp. 611–621.
- [20] S. Kazemzadeh, V. Ordonez, M. Matten, and T. Berg, "ReferItGame: Referring to objects in photographs of natural scenes," in *EMNLP*, 2014, pp. 787–798.
- [21] R. Krishna, Y. Zhu, O. Groth, J. Johnson, K. Hata, J. Kravitz, S. Chen, Y. Kalantidis, L.-J. Li, D. A. Shamma, M. S. Bernstein, and L. Fei-Fei, "Visual Genome: Connecting language and vision using crowdsourced dense image annotations," *International Journal of Computer Vision*, vol. 123, no. 1, pp. 32–73, 2017.
- [22] L. Yu, P. Poirson, S. Yang, A. C. Berg, and T. L. Berg, "Modeling context in referring expressions," in *ECCV*, 2016, pp. 69–85.
- [23] B. Hemanthage, H. Bilen, P. Bartie, C. Dondrup, and O. Lemon, "RECENTFormer: Referring expression comprehension with varying numbers of targets," in *EMNLP*, 2024, pp. 21 784–21 798.
- [24] A. Nicolson, J. Dowling, and B. Koopman, "Improving chest X-ray report generation by leveraging warm starting," *Artificial Intelligence in Medicine*, vol. 144, p. 102633, 2023.
- [25] A. Nicolson, S. Zhuang, J. Dowling, and B. Koopman, "The impact of auxiliary patient data on automated chest X-ray report generation and how to incorporate it," in *ACL*, 2025, pp. 177–203.
- [26] F. Liu, X. Wu, S. Ge, W. Fan, and Y. Zou, "Exploring and distilling posterior and prior knowledge for radiology report generation," in *CVPR*, 2021, pp. 13 753–13 762.
- [27] C. Wu, X. Zhang, Y. Zhang, W. Xie, and Y. Wang, "Towards generalist foundation model for radiology by leveraging web-scale 2D&3D medical data," *Nature Communications*, vol. 16, no. 1, p. 7866, 2025.
- [28] H.-Y. Zhou, J. N. Acosta, S. Adithan, S. Datta, E. J. Topol, and P. Rajpurkar, "MedVersa: A generalist foundation model for medical image interpretation," *arXiv:2405.07988 [cs.CV]*, 2024.
- [29] A. Nicolson, J. Dowling, D. Anderson, and B. Koopman, "Longitudinal data and a semantic similarity reward for chest X-ray report generation," *Informatics in Medicine Unlocked*, vol. 50, p. 101585, 2024.
- [30] X. Zhang, C. Wu, Z. Zhao, J. Lei, W. Tian, Y. Zhang, W. Xie, and Y. Wang, "Development of a large-scale grounded vision language dataset for chest CT analysis," *Scientific Data*, vol. 12, no. 1, p. 1636, 2025.
- [31] L. Luo, B. Tang, X. Chen, R. Han, and T. Chen, "VividMed: Vision language model with versatile visual grounding for medicine," in *NAACL*, 2025, pp. 1800–1821.
- [32] K. He, X. Zhang, S. Ren, and J. Sun, "Deep residual learning for image recognition," in *CVPR*, 2016, pp. 770–778.
- [33] T. Sounack, J. Davis, B. Durieux, A. Chaffin, T. J. Pollard, E. Lehman, A. E. W. Johnson, M. McDermott, T. Naumann, and C. Lindvall, "BioClinical ModernBERT: A state-of-the-art long-context encoder for biomedical and clinical NLP," *arXiv:2506.10896 [cs.CL]*, 2025.
- [34] A. E. Johnson, T. J. Pollard, S. J. Berkowitz, N. R. Greenbaum, M. P. Lungren, C.-y. Deng, R. G. Mark, and S. Horng, "MIMIC-CXR, a de-identified publicly available database of chest radiographs with free-text reports," *Scientific Data*, vol. 6, no. 1, p. 317, 2019.
- [35] Meta AI, "Introducing Meta Llama 3," <https://ai.meta.com/blog/meta-llama-3/>, 2024.
- [36] I. Loshchilov and F. Hutter, "Decoupled weight decay regularization," in *ICLR*, 2017.
- [37] A. Nicolson, J. Liu, J. Dowling, A. Nguyen, and B. Koopman, "e-Health CSIRO at RRG24: Entropy-augmented self-critical sequence training for radiology report generation," in *Proceedings of the 23rd Workshop on Biomedical Natural Language Processing*, 2024, pp. 99–104.